ORIGINAL PAPER

Electronic and Magnetic Properties of the BaTiO$_3$/LaMnO$_3$ Interface: a DFT Study

Irina Piyanzina[1] · **Rinat Mamin**[1]

Abstract

The electronic and magnetic properties of the BaTiO$_3$/LaMnO$_3$ interface were investigated by means of ab initio calculations within the density functional theory (DFT). An impact of the thickness of the ferroelectric overlayer on the interface properties was analysed through the spin-polarized density of states. It was been shown that the band gap decreases with increasing the thickness of ferroelectric overlayer, approaching zero.

Keywords Ferroelectric interface · Magnetoelectric coupling · DFT

1 Introduction

The LaAlO$_3$/SrTiO$_3$ (LAO/STO) heterostructure has been extensively studied over the past last 20 years after the two-dimensional gas (2DEG) observation at the interface of this system [1]. It has been found that the conducting state coexists with the magnetic state. The arising magnetic order in the LAO/STO system is the subject of intensive discussion [2, 3]. From ab initio calculations, it was revealed that the bare heterostructure is non-magnetic, and magnetic ordering is associated with the formation of defects, in particular, oxygen vacancies at the interface and/or the surface [2, 4]. The arising magnetization is weak, and according to Ref. [4] the maximal magnetic moment per Ti atom is 0.232 μ_B.

Besides, below 300 mK LAO/STO system passes into the superconducting state [5]. Recently, in one of our previous studies, using ab initio, it was demonstrated that the use of a high-temperature superconductor

(PCHTSC) La$_2$CuO$_4$ as a substrate and ferroelectric oxide BaTiO$_3$ in the heterostructure as an overlayer can lead to a conducting state located predominantly in the interfacial LCO layer. Lately, a high-temperature quasi-two-dimensional superconducting state has been observed in the Ba$_{0.8}$Sr$_{0.2}$TiO$_3$/La$_2$CuO$_4$ heterostructure with T_c=30 K [6]. This T_c is 100 times larger than T_c in LAO/STO [5].

An experimental observation of conducting state was also realized in the Ba$_{0.8}$Sr$_{0.2}$TiO$_3$/LaMnO$_3$ system [7]. Such a heterostructute consists of a ferromagnet, which can serve as a source of magnetic state, and a ferroelectric, which can be used as a tool for electron doping [8, 9]. Consequently, in the LaMnO$_3$/BaTiO$_3$ (LMO/BTO) heterointerface it is expected to have the interfacial magnetism along with conducting state. It presented paper, we investigate the possibilities of the spin-polarized 2DEG appearing in the LMO/BTO heterostructure. The essential issue is to understand the impact of the ferroelectric BTO slab thickness on the interface electronic and magnetic states. In order to do so, we investigate the BTO/LMO heterostructure with varying number of BTO overlayers and analyse the density of state spectra.

2 Calculation Details

The ab initio calculations were based on density functional theory (DFT) [10, 11]. Exchange and correlation effects were accounted for by the generalized gradient approximation (GGA) as parametrized by Perdew, Burke, and Ernzerhof (PBE) [12]. The Kohn-Sham equations were solved with projector-augmented-wave (PAW) potentials and wave functions [13] as implemented in the Vienna Ab-Initio Simulation Package (VASP) [14–16], which is part of the MedeA® software of Materials Design [17]. Specifically, we

✉ Irina Piyanzina
i.piyanzina@gmail.com

1 Zavoisky Physical-Technical Institute, FIC KazanSC of RAS, 420029 Kazan, Russia

Fig. 1 Density of states spectrum for the bulk A-AFM LaMnO$_3$ along with the corresponding unit cell structure
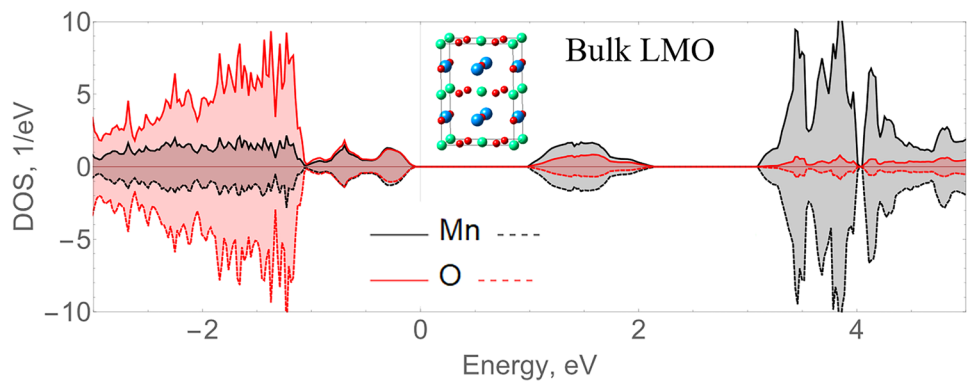
used a plane-wave cutoff of 400 eV. The force tolerance was 0.05 eV/Å and the energy tolerance for the self-consistency loop was 10^{-5} eV. The Brillouin zones were sampled using Monkhorst-Pack grids [18] including $5 \times 5 \times 1$ **k**-points. A set of calculations was carried out with a $+U$ correction applied to Mn 3d, Ti 3d and La 4f states. A simplified Dudarev approach was used [20]: the U values of 4 eV for Mn, 2 eV for Ti and 8 eV for La states were applied. The choice of U-values for Ti and La were based on our previous research [19], whereas for Mn was taken from Ref. [21].

The heterostructures were modelled by a central region of LaMnO$_3$ comprising 11 atomic layers with LaO termination on both sides and varying number of BaTiO$_3$ overlayers with TiO$_2$ termination towards the central slab and BaO surface termination also on both sides. In order to avoid interaction of the surfaces and slabs with their periodic images, $\approx$ 20 Å-wide vacuum region was added.

3 Results

3.1 Bulk Components

First, the parent materials of the heterointerface have been checked separately in bulk geometry to ensure the reproducibility of the results obtained by the method and computational parameters used in the present research. Starting

from the experimental structure of bulk LaMnO$_3$, the lattice constants and atomic positions were fully relaxed.

To realize the spin-dependent switching effect, which was mentioned in the introduction, it was suggested to replace the FM material with AFM [8]. The spin-polarized density of states (DOS) plot for the A-AFM LMO in bulk configuration in presented in Fig. 1. The bulk LMO is a semiconductor with an O 2p dominated valence band, with Mn 3d contribution. The calculated band gap and magnetic moment of the Mn atom equal 1.349 eV and 3.832 μ_B, respectively. These values agree well with experimental values of 1.7 eV and $3.7 \pm 0.1 \mu_B$, respectively [22]. Based on this comparison, we concluded that the chosen value of the U parameter can yield relatively correctly both the energy gap and the magnetization. Besides, the calculated cell parameters shown in Table 1 turned out to be close to experimental values [23] as well as to previous ab initio studies, for example Ref. [24].

BaTiO$_3$ is one of the most well-known ferroelectric, which has a ferroelectric polarization in a tetragonal system with moderate polarization of 26 μC/cm^2 [26]. The calculated values of energy per unit cells, band gaps, oxygen displacements and polarization for the cubic, tetragonal and orthorhombic phases are presented in Table 2. All calculated values agree well with the experimental data. The experimental band gap is higher than the computed one, but the difference is reasonable for DFT. For the purpose of this work, we are interested in the phases with spontaneous polarization, so we will focus on the tetragonal structure

Table 1 Calculated lattice constants in Å of the bulk LaMnO$_3$ and BaTiO$_3$, and of a rotated by 45° along z-axis BaTiO$_3$ unit cell in order to merge with the LaMnO$_3$ unit cell. The last row lists the BaTiO$_3$/LaMnO$_3$ supercell lattice constants. Experimental data is presented as well for comparison

	a	b	c
LMO	5.709	5.675	8.018
Expt. [23]	5.742	5.532	7.669
BTO	3.986	3.986	4.014
Expt. [25]	3.992	3.992	4.036
BTO ($\times\sqrt{2}$)	5.637	5.637	4.014
Supercell	5.709	5.675	50

Table 2 Calculated energy (E) per unit cell, c/a ratio, the band gaps (ε), displacements of Ti atoms with respect to the O planes ($\triangle$) and polarization **P** in μC/cm^2 of the cubic, tetragonal and orthorhombic phases of bulk BaTiO$_3$. Experimental values are given for the tetragonal phase

Phase	c/a	ε, eV	$\triangle$, Å	**P**
Cubic	1	2.169	0	0
Tetragonal	1.007	2.249	0.13	31
Expt.	1.010 [27]	3.27 [28]	0.15 [27]	26 [26]
Orthorhombic	1.428	2.259	0.09	

of BTO. The calculated lattice parameters, together with experimental ones, are listed in Table 1. The calculated density of state spectrum for the bulk BTO is given in Fig. 2.

3.2 LaMnO₃/BaTiO₃ Heterostructure

In order to merge BTO with LMO so that the polarization is parallel to the easy axis of antiferromagnet, the BTO unit cell has to be rotated by 45° along the z-axis. As listed in Table 1 $a_{BTO} \times \sqrt{2}$ is very close to the a_{LMO} and b_{LMO} cell parameters. The resulting supercell with two BTO overlayers is presented in Fig. 3 a, where the right half of the unit cell is presented without the full vacuum region. The structure has been fully optimized.

Performed structural optimization resulted in an insignificant shift of Ti atoms out of the oxygen planes (Δz_{Ti-O}). For a heterostructure with two BTO overlayers Δz_{Ti-O} distances within the interfacial layer equal to −0.046 Å and 0.247 Å, within the surface layer shifts are less significant and equal to 0.049 Å and 0.101 Å, respectively. Except for one, all movements of Ti are directed towards the surface, which leads to the total polarization predominantly towards the surface. Such a structural reconstruction leads to an electronic rearrangement, which is reflected in the DOS spectra shown in Fig. 4a–d for varying number of BTO layers. As the number of BTO overlayers increases, the band gap decreases from 0.47 eV for heterostructure with one BTO overlayer to 0.113 eV with four. This decay of the band gap with the number of overlayers differs from the linear dependence of LAO/STO as shown in Fig. 5. Indeed, the band gap decreases with an increase in the number of LAO overlayers in LAO/STO, which is associated with an increase in the field directed towards the surface. As soon as this field exceeds the field arising due tin according to our o the structural relaxation, the LAO/STO system becomes conductor. This happens above 4 LAO overlayers according to our previous ab initio research [4]. On the contrary, in the LMO/BTO heterostructure without polar overlayers the field towards the surface originates from the ferroelectric
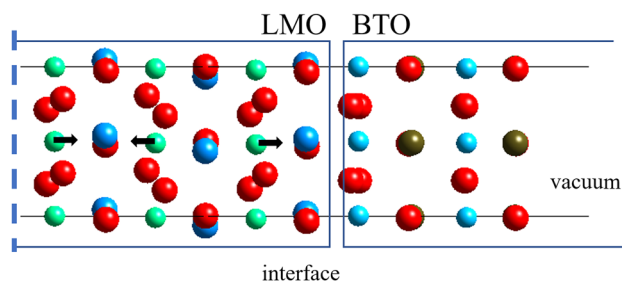

Fig. 3 The fully optimized half-right structure of the LMO/2BTO heterointerface. The supercell is displayed without the vacuum region, which was 20Å. The arrows indicate the magnetic moments directions in the LMO slab

polarization. Since the slope in Fig. 5 for LMO/BTO is smaller, it is clear that the ferroelectric field is weaker and conductivity occurs with more overlayers. Note, that in experiments [7] the thickness of the ferroelectric film was about 350 nm, and based on the asymptotics of our calculations it is expected that the band gap completely disappears at this thickness.

Indeed, the structural relaxation plays a crucial role in electron transport in heterostructures. In the LAO/STO heterostructure with no relaxation due to the sequence of positive/negative atomic layers in the LAO film the potential build-up and electrostatic field arise towards the surface of the slab. Leading to the cross of interface Ti states and O surface states at the Fermi-level. Performed structural relaxation leads to the Ti out of oxygen planes shifts and consequently oppositely directed field. As soon as the field due to the charged layers exceeds the field due to the structural relaxation (which happens with more than 4 LAO layers), electrons flow from the surface to the interface and the conductivity takes place. Now, in the LMO/BTO heterostructure situation is different. With no relaxation, there is no potential build-up in the ferroelectric layer since all layers are neutral in the simple ionic limit. According to calculations "ideal" LMO/BTO heterostructures are

Fig. 2 Density of states spectrum for the bulk BaTiO₃ along with the corresponding unit cell structure
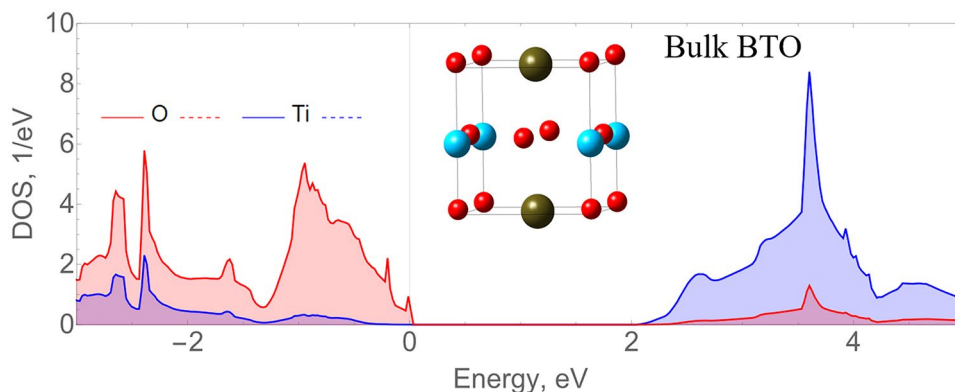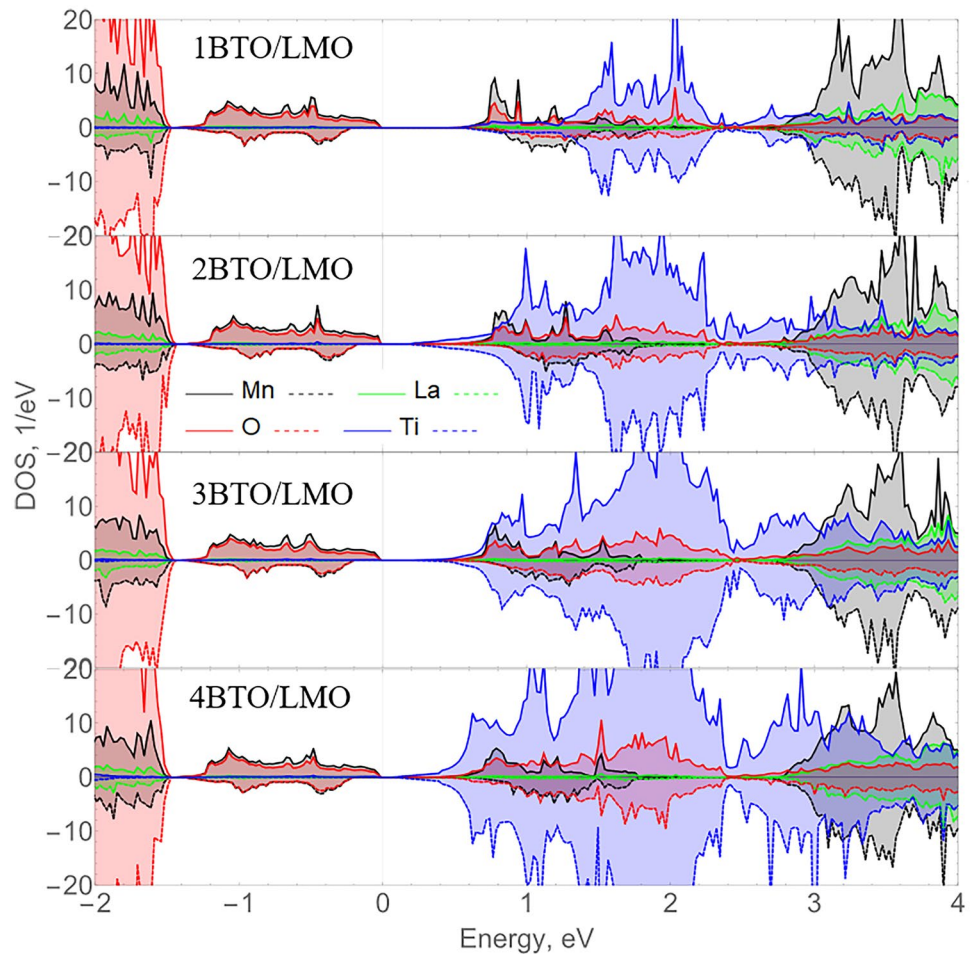
Fig. 4 Atom-resolved density of states spectra for the hetero-structure with varying number (1–4) BTO overlayers

metals with any number of BTO. Relaxation results in the movements of Ti upwards leading to the optimization field directed towards the surface. In this field electrons move against it towards the LMO.

Finally, the LMO/BTO system possesses relatively high total magnetization due to the odd number of MnO layers with magnetic moment per Mn equal to 3.8 μ_B. Ferromagnetic magnetization should increase with increasing the electron doping.

Fig. 5 Calculated band gap versus the number of BTO overlayers in LMO/BTO hetero-structure along with analogous dependence for LAO/STO systems for comparison
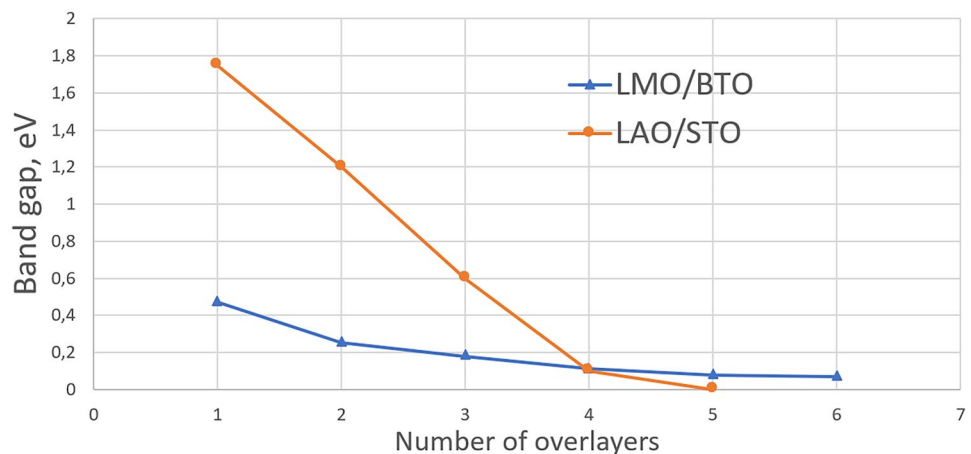
4 Conclusions

In the present paper, by means of DFT+U calculation the electronic and magnetic properties of bulk $LaMnO_3$ and $BaTiO_3$, as well as LMO/BTO heterostructure have been demonstrated. Within the framework of the chosen approach and computational parameters, it was confirmed that the bulk components of the heterostructure are non-conductors.

In the heterostructure geometry, the decrease in the band gap with an increase in the number of BTO overlayers was demonstrated. It was found that the curve tends to zero, but the system remains semiconductor up to six BTO overlayers. It means that the conducting state arises with a larger number of ferroelectric overlayers, which is consistent with experiment from Ref. [7], where the thickness of ferroelectric $Ba_{0.8}Sr_{0.2}TiO_3$ film was much larger. It should be noted that in the paper we assume that adding Sr atoms into the supercell would not affect the band gap behaviour significantly and the dependence would be the same for non-stochiometric heterostructure. Our assumption was based on the fact that DOS of bulk $Ba_{0.8}Sr_{0.2}TiO_3$ and BTO look very similar and the band gaps are very close, as we found from calculations within same level of theory. That is why for our purpose we kept the system as simple as possible.

Finally, It was shown that the LMO/BTO system possesses relatively high total magnetization, which is expected to increase with increasing the electron doping.

Declarations

Conflict of Interest The authors declare no competing interests.

References

1. Ohtomo, A., Hwang, H.Y.: Nature **427**, 423–426 (2004)
2. Pavlenko, N., Kopp, T., Tsymbal, E.Y., Mannhart, J., Sawatzky, G.A.: Phys. Rev. B **86**(6), 064431 (2012)
3. Michaeli, K., Potter, A.C., Lee, P.A.: Phys. Rev. Lett. **108**(11), 117003 (2012)
4. Piyanzina, I.I., Eyert, V., Lysogorskiy, Yu.V., Tayurskii, D.A., Kopp, T.: J. Phys.: Condens. Matter **31**(29), 295601 (2019)
5. Reyren, N., Thiel, S., Caviglia, A.D., Fitting Kourkoutis, L., Hammerl, G., Richter, C., Schneider, C.W., Kopp, T., Retschi, A.S., Jaccard, D., Gabay, M., Muller, D.A., Triscone, J.M., Mannhart, J.: Science **317**, 1196 (2007)
6. Pavlov, D.P., Zagidullin, R.R., Mukhortov, V.M., Kabanov, V.V., Adachi, T., Kawamata, T., Koike, Y., Mamin, R.F.: Phys. Rev. Lett. **122**, 237001 (2019)
7. Pavlov, D.P., Piyanzina, I.I., Muhortov, V.I., Balbashov, A.I., Tauyrskii, D.A., Garifullin, I.A., Mamin, R.F.: JETP Lett. **106**, 440–444 (2017)
8. Weng, Y., Niu, W., Huang, X., An, M., Dong, Sh.: Phys. Rev. B **103**, 214101 (2021)
9. Kabanov, V.V., Piyanzina, I.I., Lysogorskiy, Yu.V., Tayurskii, D.A., Mamin, R.F.: Mater. Res. Express **7**, 055020 (2020)
10. Hohenberg, P., Kohn, W.: Phys. Rev. **136**, B864 (1964)
11. Kohn, W., Sham, L.J.: Phys. Rev. **140**, A1133 (1965)
12. Perdew, J.P., Burke, K., Ernzerhof, M.: Phys. Rev. Lett. **77**, 3865 (1996)
13. Blöchl, P.E.: Phys. Rev. B **50**, 17953 (1994)
14. Kresse, G., Furthmüller, J.: Comp. Mat. Sci. **6**, 15 (1996)
15. Kresse, G., Furthmüller, J.: Phys. Rev. B **54**, 11169 (1996)
16. Kresse, G., Joubert, D.: Phys. Rev. B **59**, 1758 (1999)
17. MedeA version 3.4; MedeA is a registered trademark of Materials Design, Inc., San Diego, USA
18. Monkhorst, H.J., Pack, J.D.: Phys. Rev. B **13**, 5188 (1976)
19. Piyanzina, I.I., Kopp, T., Lysogosrkiy, Yu.V., Tayurskii, D., Eyert, V.: J. Phys.: Condens. Matter **29**, 095501 (2017)
20. Dudarev, S.L., Botton, G.A., Savrasov, S.Y., Humphreys, C.J., Sutton, A.P.: Phys. Rev. B **57**, 1505 (1998)
21. Wang, L., Maxisch, T., Ceder, G.: Phys. Rev. B **73**, 195107 (2006)
22. Saitoh, T., Bocquet, A.E., Mizokawa, T., Namatame, H., Fujimori, A., Abbate, M., Takeda, Y., Takano, M.: Phys. Rev. B **51**, 20 (1995)
23. Sawada, H., et al.: Phys. Rev. B **56**, 12154 (1997)
24. Ciucivara, A., Sahu, B., Kleinman, L.: Phys. Rev. B **77**, 092407 (2008)
25. Landolt Brnstein, Crystal and Solid State Physics, p.67. New Series, Group III, Vol. 16a Springer, Berlin (1981)
26. Subarao, E.C.: Ferroelectrics **5**, 267 (1973)
27. Shirane, G., Danner, H., Pepinsky, R.: Phys. Rev. **105**, 856 (1957)
28. Wemple, S.: Phys. Rev. B **2**, 2679 (1970)